International Conference on Green Energy & Environmental Engineering (GEEE-2018)
Proceedings of Engineering and Technology – PET
Vol.38 pp.64-68

Application of Direct Power Control in Wind Energy Conversion System

K. Bedoud[1,2], A. Rhif[3], T. Bahi[2], H. Merabet[1], A. Bouazdia[1]

[1]*Research Center in Industrial Technologies CRTI, ex CSC, BP 64 Cheraga, Algeria.*
[2] *Automatic Laboratory and Signals, BadjiMokhtar University, Annaba, Algeria*
[3] *Laboratory of Advanced Systems (Polytechnic School of Tunisia)University of Carthage*

[1]k.bedoud@crti.dz

Abstract*— This paper describes the performance evaluation of the direct power control for a three-phase pulse with modulation inverter fed by a variable speed wind energy conversion system. This, to ensure a maximum power point tracking of a wind. Proposed direct power control strategy is implemented in the d-q reference frame. The system modeling and control scheme are implemented on Matlab/Simulink. The simulation results show that the use of the direct Power Control provide nearly sinusoidal input wave form current, constant switching frequency operation, regulation of unity power factor in the connection of the grid side converter with the grid and the maintain of the DC-link voltage constant. Finely, the results verify the validity and effectiveness of the proposed control.

Keywords—**Renewable energies, wind energy conversion system, direct power control, simulation.**

I. INTRODUCTION

Nowadays, energy is one of the central and foremost grand challenges facing our society today. Particularly, wind energy is becoming one of the most important renewable energy sources; it will likely provide the main renewable contributions to the growing need for clean energy [1], [2]. Variable speed Wind Energy Conversion System (WECS) have become the industry standard because of their advantages over fixed speed ones such as improved energy capture, better power quality. With the growing of power electronic devices, three-phase rectifiers have been widely applied to wind energy system. A three-phase voltage source converter offers many advantages, namely bidirectional power flow, low harmonic distortion of input currents and regulation of input power factor to unity, low switch voltage stress and low switching frequency [3],[4]. In recent years, different strategies have been proposed for controlling Pulse With Modulation (PWM) converter. The main goal of these control strategies is to obtain the high power control and sinusoidal current estimated flux signal used in the control system [5]. In this paper, the Direct Power Control (DPC) is considered, so, the converter switching states are selected by a switching table based on the instantaneous errors between the commanded and estimated values of the active and reactive power, and voltage position vector [6]. For such several advantages, the DPC has attracted attention and a lot of curiosity of many researchers.

The present paper is organized as follow: In section II, wind energy conversion system model is presented. After, the principle of direct power control is explained in Section III. The rectifier control using direct power control is programmed under Matlab/Simulink environment and the analyses of the performances are given in Section IV. Finally, simulation results and conclusion are presented.

II. WIND ENERGY CONVERSION SYSTEM MODEL

Wind energy conversion system considered in this work is shown in figure 1. It includes the wind turbine, gearbox, Double Fed Induction Generator (DFIG), and back-to-back converters whereas the rotor is fed by back-to-back bidirectional converter and the stator is directly connected to the grid. This system allows conversion of the wind energy through the turbine to the three-phase DFIG. This energy is transmitted directly through a bridge rectifier and inverter to the electrical network.

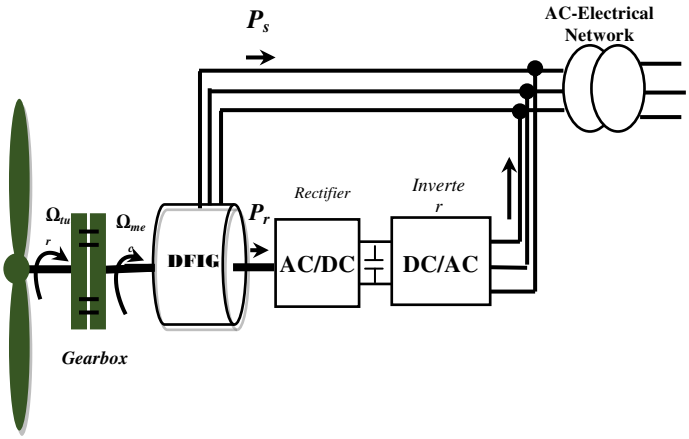


Fig.1. Schematic diagram of wind energy conversion system

II.1 Turbine modelling

Wind power P_v and the aerodynamic power $P_a$captured by the wind turbine are given by:

$$P_v = C_p(\lambda, \beta).\frac{\rho.Sv^2}{2} \quad (1)$$

Where,

Copyright IPCO-2018
ISSN 2356-5608

C_p: power coefficient;
ρ: air density (1.25 Kg/m3);
v: wind speed;
R : turbine rayon.

The tip-speed ratio (λ) is given by:

$$\lambda = \frac{R.\Omega_{tur}}{V} \quad (2)$$

Power coefficient can be approximated by the following equation:

$$C_p(\lambda,\beta) = 0.22\left(\frac{116}{\lambda_i} - 0.4\beta - 5\right)e^{\frac{-12.5}{\lambda_i}} \quad (3)$$

$$\frac{1}{\lambda_i} = \frac{1}{\lambda+0.08\beta} - \frac{0.035}{1+\beta^3} \quad (4)$$

So, the aerodynamic torque is expressed by:

$$T_{tur} = \frac{P_{tur}}{\Omega_{tur}} = C_p(\lambda,\beta).\frac{\rho.S.V^3}{2}.\frac{1}{\Omega_{tur}} \quad (5)$$

The mechanical equation of the system is characterized as follow:

$$J\frac{d\Omega_{mec}}{dt} = T_{mec} - T_{em} - f\Omega_{mec} \quad (6)$$

Figure 2 shows the relation between the turbine power and rotor speed for different wind speed. We can deduce that there is one value which ensures maximum power captured from the wind for each wind speed value.

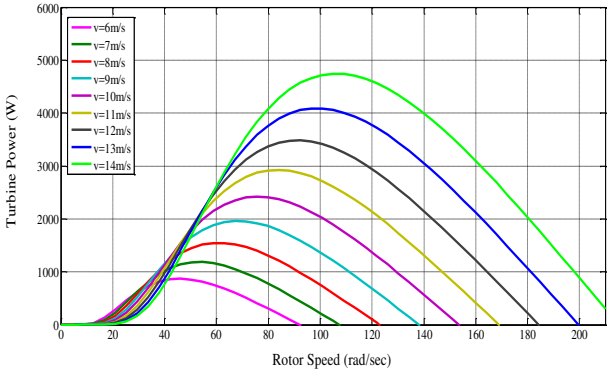


Fig.2 Turbine power versus rotor speeds and wind speed

II.2 Modeling of the DFIG

The DFIG model is obtained in synchronous d-q reference frame where the d-axis is aligned with the stator flu vector position (Fig. 3). The influence of the stator resistance can be neglected and the grid is supposed stable with voltage v_s and synchronous angular frequencyω_s . Consequently [7]:

$$\begin{cases} V_{sd} = \frac{d\varphi_{sd}}{dt} = 0 \\ V_{sq} = \omega_s.\varphi_{sd} = V_s \end{cases} \quad (7)$$

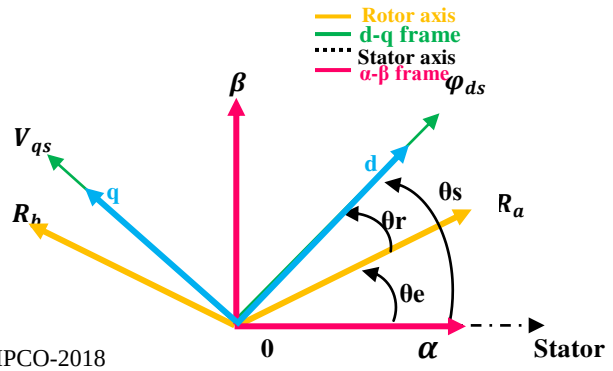


Fig.3 Stator field oriented control technique

Hence, the DFIG mathematical model can be written as follow:

$$\begin{cases} V_{sd} = \frac{R_s}{L_s}\varphi_{sd} - \frac{R_s}{L_s}L_m i_{rd} \\ V_{sq} = -\frac{R_s}{L_s}L_m i_{rq} + \omega_s\varphi_{sd} \end{cases} \quad (8)$$

$$\begin{cases} V_{rd} = R_r i_{rd} + \sigma.L_r\frac{di_{rd}}{dt} + e_{rd} \\ V_{rq} = R_r i_{rq} + \sigma.L_r\frac{di_{rq}}{dt} + e_{rq} + e_\varphi \end{cases} \quad (9)$$

$$\begin{cases} \varphi_{rd} = \left(L_r - \frac{M^2}{L_s}\right)i_{rd} + \frac{MV_s}{\omega_s L_s} \\ \varphi_{rq} = \left(L_r - \frac{M^2}{L_s}\right)i_{rq} \end{cases} \quad (10)$$

$$\begin{cases} P_s = -\frac{V_s.M}{L_s}.i_{rq} \\ Q_s = \frac{V_s^2}{L_s\omega_s} - \frac{M.V_s}{L_s}.i_{rd} \\ P_r = g.\frac{V_s.M}{L_s}.i_{rq} \\ Q_r = g.\frac{V_s.M}{L_s}.i_{rd} \end{cases} \quad (11)$$

With:

$$\begin{cases} e_{rd} = -\sigma.L_r.\omega_r.i_{rq} \\ e_{rq} = \sigma.L_r.\omega_r.i_{rd} \\ e_\varphi = \omega_r.\frac{M}{L_s}.\varphi_{sd} \\ \sigma = 1 - \left(\frac{M}{\sqrt{L_s L_r}}\right)^2 \end{cases} \quad (12)$$

From equation (13), we can deduce that the active and reactive powers can reach decoupling control. The electromagnetic torque is as follows :

$$T_{em} = -P.\frac{M}{L_s}\varphi_{sd}.i_{rq} \quad (13)$$

II.3 Modeling of three-phase PWM converter

The mathematic model of the converter can be expressed in matrix form with following equations [8]:

$$\begin{bmatrix} v_{sa} \\ v_{sb} \\ v_{sc} \end{bmatrix} = R\begin{bmatrix} i_a \\ i_b \\ i_c \end{bmatrix} + L\frac{d}{dt}\begin{bmatrix} i_a \\ i_b \\ i_c \end{bmatrix} + \begin{bmatrix} v_a \\ v_b \\ v_c \end{bmatrix} \quad (14)$$

The voltages v_a, v_b and v_c are defined as:

Copyright IPCO-2018
ISSN 2356-5608

$$\begin{cases} v_a = \frac{v_{dc}}{3}(2S_a - S_b - S_c) \\ v_b = \frac{v_{dc}}{3}(-S_a + 2S_b - S_c) \\ v_c = \frac{v_{dc}}{3}(-S_a - S_b + 2S_c) \end{cases} \quad (15)$$

Where the switching states can be represented as:

$$S_k = \begin{cases} +1, \overline{S_k} = -1 \\ -1, \overline{S_k} = +1 \end{cases} \text{ for } k = a, b, c. \quad (16)$$

The DC-link current can be written by the following relation:

$$c\frac{dv_{dc}}{dt} = S_a i_a + S_b i_b + S_c i_c - S_c i_l \quad (17)$$

III. DPC Control Strategy

The aim is to directly control active and reactive power in a PWM rectifier. Indeed, the errors between the reference values of the instantaneous active and reactive powers and their measurements are introduced in two hysteresis comparators which determine, with the help of a switching table and the value of the sector where the mains voltage is located, the semiconductors switching state. The active and reactive powers are directly controlled by selecting the optimal switching state and with hysteresis controllers. Furthermore, the switching table principle is based on the position of the instantaneous active and reactive powers errors variations "Δp" and "Δq"and the position of mains voltage vector, where the reference of the instantaneous active power is achieved with the PI controller by regulating the DC-link voltage. In this section, direct power control scheme that uses multistage band hysteresis comparator and a switching table is proposed. The reference frame is divided into six sectors (6) as shown in Fig. 4, which the sectors can be numerically expressed as:

$\frac{-\pi}{6} + (k-1)\frac{\pi}{3} \le \theta(k) \le \frac{\pi}{6} + (k-1)\frac{\pi}{3}$ Or, k=1, 2….6

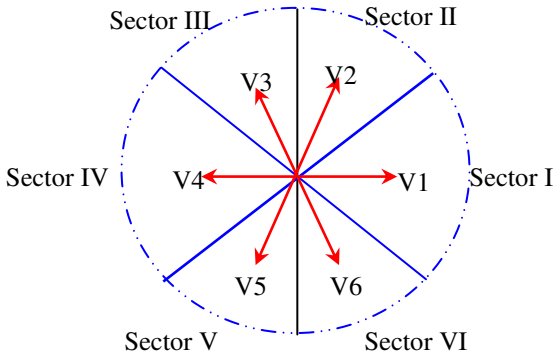


Fig.4. Voltage vectors sectors

The errors between the reference and the actual power Δp and Δq were quantified into two levels "0" and "1" by a multistage band hysteresis comparator. The following algorithm describes two-stage hysteresis regulators for instantaneous active and reactive power. The DPC (see Fig.5) consists of selecting a control vector from a switch table. This last is based on the numerical errors S_p, S_q which are limited by a hysteresis band, as well as on the angular position of the voltage at the connection point of the load with the network. The plane (α, β) is divided into six sectors to determine the work sector. The choice of the switching mode of the rectifier is realized so that the error between the reference value of the instantaneous active power, P_{ref}, and the measured value p, falls within the hysteresis band $2.\Delta P$. In the same way, the reactive power error must remain in the hysteresis band $2\Delta.q$. To achieve this objective, the instantaneous active and reactive powers errors are processed by two two-level hysteresis comparators, whose outputs (d_p, d_q) are set to 1 when the control variable (p, q) has to be increased and to 0 when the control variable must remain unchanged or must decrease [9].

$$\begin{cases} -H_q \le \Delta q \le H_q & and \quad \frac{d\Delta q}{dt} > 0, & S_q = 0 \\ -H_q \le \Delta q \le H_q & and \quad \frac{d\Delta q}{dt} < 0, & S_q = 1 \\ \Delta q < -H_q \ , & & S_q = 0 \\ \Delta p > H_q \ , & & S_q = 1 \end{cases} \quad (18)$$

$$\begin{cases} -H_p \le \Delta p \le H_p & and \quad \frac{d\Delta p}{dt} > 0, & S_p = 0 \\ -H_p \le \Delta p \le H_p & and \quad \frac{d\Delta p}{dt} < 0, & S_p = 1 \\ \Delta p < -H_p \ , & & S_p = 0 \\ \Delta p > H_p \ , & & S_p = 1 \end{cases} \quad (19)$$

Where H_p and H_q are the hysteresis band of active and reactive powers comparators, respectively. Table I presents the signs variation of the instantaneous active and reactive power for each input voltage vector according to the sector (j = 1, 6). By choosing the appropriate output vector, it is possible to select the active and reactive power variation signs independently. An analysis of the table shows that in some cases there are several possibilities of obtaining the same increment (the same signs of Δp and Δq are obtained by applying different vectors). In these cases, the choice of the voltage vector is that which causes the lowest power variation. Only four voltage vectors: v(k-1), v(k), v(k+1) and v(k+2) Meet this criterion.

TABLE I
Signs Variation of Active and Reactive Power

Δp	Δq	e
0	0	V(k)
0	1	V(k+1)
1	0	V(k-1)
1	1	V(k+2)

The voltage vector used are : $V_0(000)$, $V_1(100)$, $V_2(110)$, $V_3(010)$, $V_4(011)$, $V_5(001)$, $V_6(101)$, $V_7(111)$, where only six vectors are activated. Binary number in the brackets shows switching states in the phase sequence a, b and c.

Copyright IPCO-2018
ISSN 2356-5608

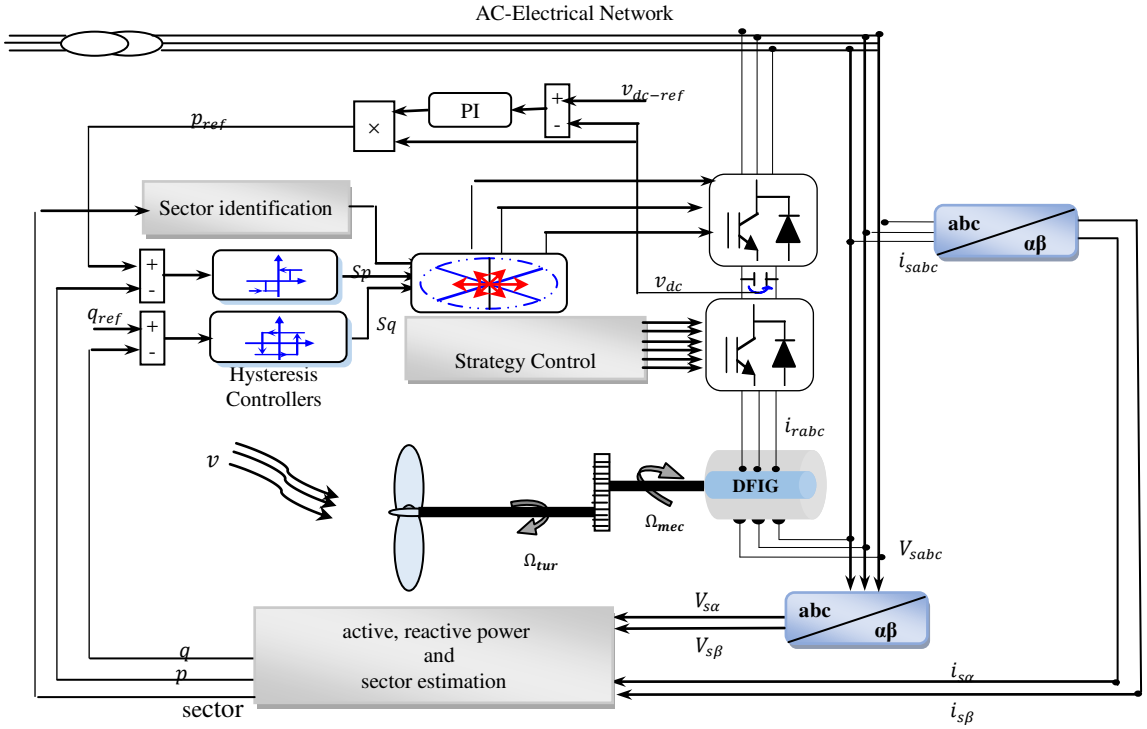


Fig.5. Schematic diagram of the proposed control algorithm

TABLE II
SSWITCHING TABLE FOR DIRECT POWER CONTROL

S_p	S_q	Sec1	Sec2	Sec3	Sec4	Sec5	Sec6
0	0	V6	V1	V1	V2	V2	V3
	1	V1	V2	V2	V3	V3	V4
1	0	V5	V6	V6	V1	V1	V2
	1	V3	V4	V4	V5	V5	V6

The obtained results are interpreted and criticized in the following section to highlight the performance of the proposed control.

IV. SIMULATION AND RESULTS

The global system simulation (source, load, rectifier) is performed under the Matlab / Simulink environment. The controlled reactive power *is* set to zero for unity power factor operation and active power delivered from the outer PI-DC voltage controller are compared with the estimated reactive and active values, respectively. The errors are DC quantities that are delivered to PI controllers that eliminate steady state error. The output signals from PI controllers are used for switching signals generation. In order to evaluate the performances and to validate the command, the results areshown in figure 6,7,8 and 9. First, Figures 6 and 7 show, respectively, the evolutions of the active and reactive powers and their references. We notice that they follow well their magnitudes of references. First, Figures 6 and 7 shows the voltages and currents of electrical network lines.

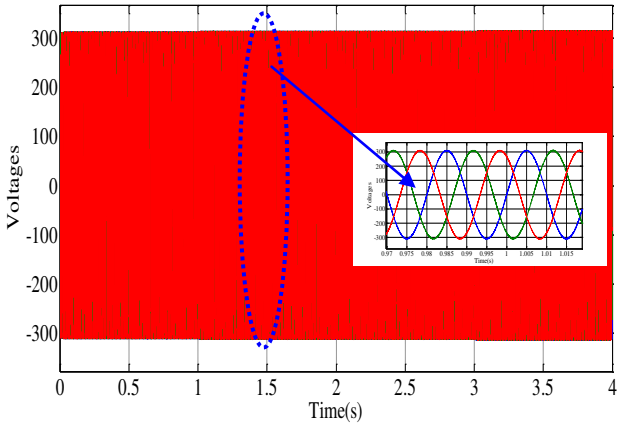


Fig.6 Voltages network

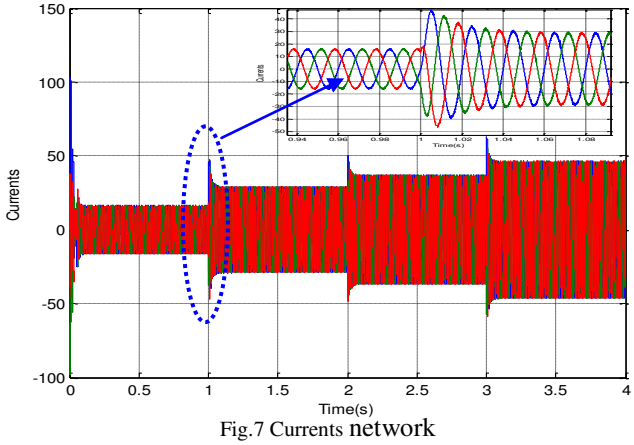


Fig.7 Currents network

Copyright IPCO-2018
ISSN 2356-5608

Figure 8 shows the reference voltage (Vref) and the continuous DC voltage (Vdc) at the output of the converter. This, for four voltages levels (600V, 800V, 900V and finally 1000V).

Figures 9 and 10 show, respectively, the evolutions of the active and reactive powers and their references. We notice that they follow well their magnitudes of references. Note that the tensions are clearly superposed.. Finally, these representations confirm that the performances are good.

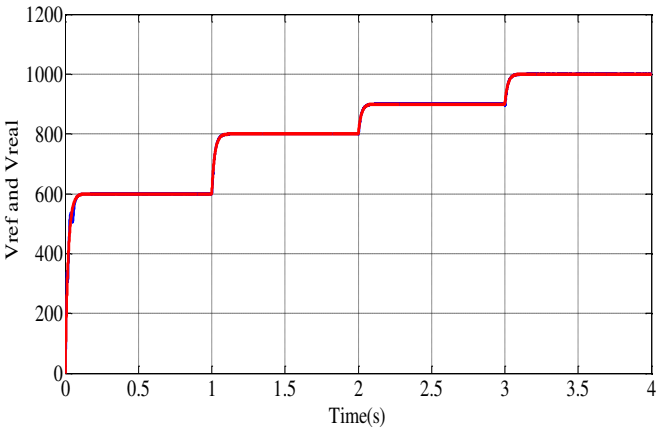


Fig.8 Reference voltage (Vref) and continuous DC voltage (Vreal)

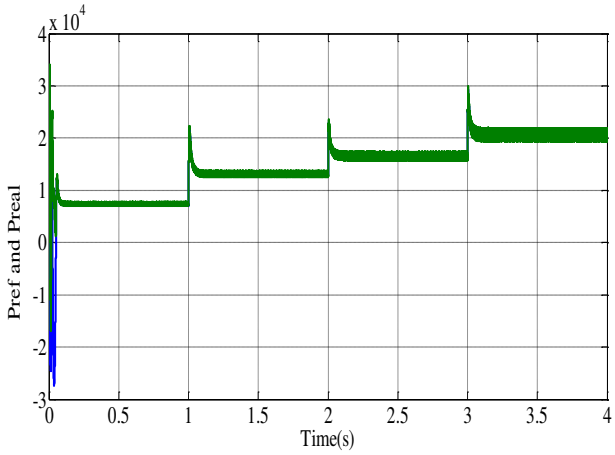


Fig.9 Reference and real active powers

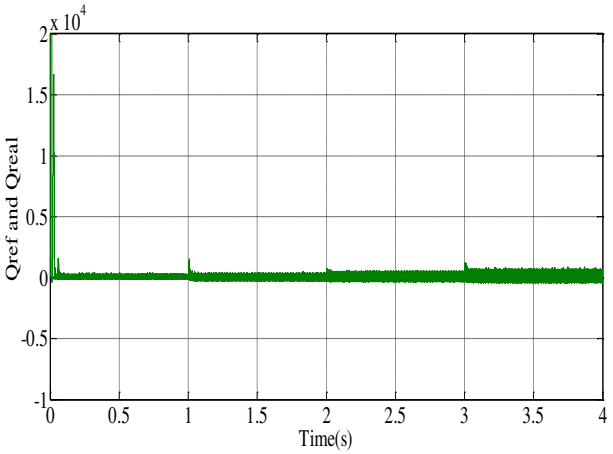


Fig.10 Reference and real reactive powers

V. Conclusion

In this article, the direct power control structure has been proposed for the side converter (GSC).This will make it possible to take advantage of the two techniques. The results of global system simulation such as speed control, indirect active and reactive powers control, DC Link voltage control give very high performances.

References

[1] G. Van Kuik and J. Peinke, *Long-term Research Challenges in Wind Energy-A Research Agenda by the European Academy of Wind Energy* vol. 6: Springer, 2016.

[2] Y. Feng and X. Yu, "Maximum Power Point Tracking Control of Wind Energy Conversion Systems," pp. 49-67, 2014.

[3] N. Muangruk and S. Nungam, "Direct Power Control of Three-phase Voltage Source Converters Using Feedback Linearization Technique," *Procedia Computer Science,* vol. 86, pp. 365-368, 2016.

[4] T. Shi, J. Wang, C. Zhang, and C. Xia, "Direct power control for three-level PWM rectifier based on hysteresis strategy," *Science China Technological Sciences,* vol. 55, pp. 3019-3028, 2012.

[5] J. Lamterkati, M. Khafallah, and L. Ouboubker, "A New DPC for Three-phase PWM rectifier with unity power factor operation," *Int. J. of Advanced Research in Electrical, Electronics and Instrumentation Engineering,* vol. 3, 2014.

[6] A. Chaoui, J. Gaubert, and A. Bouafia, "Direct power control switching table concept and analysis for three-phase shunt active power filter," *J. Electrical Systems,* vol. 9, pp. 52-65, 2013.

[7] K. Bedoud, T. Bahi, and H. Merabet, "Comparative Study of Wind Energy Conversion System Driven by Matrix Converter and AC/DC/AC Converter," in *Proceedings of the International Conference on Recent Advances in Electrical Systems*, 2016, pp. 301-306.

[8] T. A. Trivedi, R. Jadeja, and P. Bhatt, "A Review on Direct Power Control for Applications to Grid Connected PWM Converters," *Engineering, Technology & Applied Science Research,* vol. 5, pp. pp. 841-849, 2015.

[9] T. Noguchi, H. Tomiki, S. Kondo, and I. Takahashi, "Direct power control of PWM converter without power-source voltage sensors," *IEEE Transactions on Industry Applications,* vol. 34, pp. 473-479, 1998.

Copyright IPCO-2018
ISSN 2356-5608